16.5   Ferroelectricity

Many capacitor formulations are based on $BaTiO_3$, one of a number of ferroelectric substances crystallizing with the perovskite structure. Barium atoms are located at the corners of the unit cell and oxygens at the face center positions. Both barium and oxygen have ionic radii of about 1.4 Å and together they make up a face centered cubic array having a lattice parameter near 4 Å. Octahedrally coordinated titanium ions located at the center of the perovskite unit cell are the active ions in promoting ferroelectricity. The low-lying d orbitals of Ti lead to displacive phase transformations and large electronic polarizability.

On cooling from high temperature, the crystal structure of $BaTiO_3$ undergoes three ferroelectric phase transitions. All three are displacive in nature with atomic movements of 0.1 Å or less. The point symmetry changes from cubic *m3m* to tetragonal *4mm* at the Curie point of 130°C. The tetragonal state with its spontaneous polarization along [001] persists down to 0°C where it transforms to orthorhombic symmetry (point group *mm2*) as $P_{(s)}$ shifts to a [110] direction. On further cooling, the orthorhombic state transforms to rhombohedral (point group *3m*) near −90°C. The structural changes are illustrated in Fig. 16.11. A peak in the dielectric constant occurs at each of the phase transformations. Note in Fig. 16.11 that the dielectric constants along the *a* and *b* axes are larger than along the polar *c*-axis. The instability of the structure makes it easy to tilt the spontaneous polarization vector and a transverse electric field. In regard to capacitor technology, it is extremely important that the dielectric constant is high over a wide temperature range. The presence of the two lower ferroelectric phase changes ensures that the permittivity remains high below T_c.
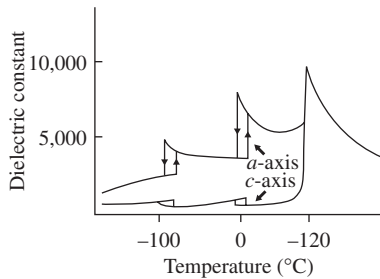
The two types of domains and domain walls are shown in Figs. 16.12–16.14. Barium titanate 180° domains with polarization along [001] and [00$\bar{1}$] are compared in Fig. 16.12. In this case the walls exhibit ferroelectric behavior but not ferroelasticity, and since there is no strain change across 180° walls, the wall orientations are not controlled by strain mismatch. There is a second criterion,
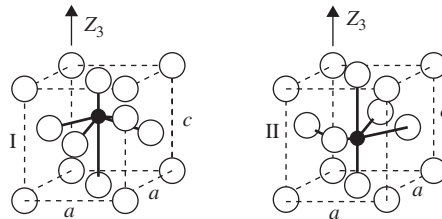
Fig. 16.11 Structural changes occurring at three ferroelectric phase transformations in $BaTiO_3$ result in large values of the dielectric constant over a wide temperature range.

Fig. 16.12 Tetragonal 180° domains in $BaTiO_3$ polarized along $\pm Z_3$. The difference in free energy shows that the walls can be driven electrically with fields along Z_3 but not with mechanical stress.
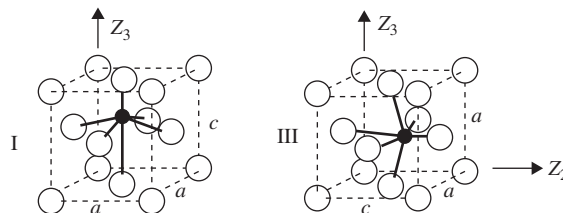
Fig. 16.13 Crystal structure drawings and free energy terms for two 90° domains polarized along Z_2 and Z_3. Mechanical stresses and electric fields are both effective in moving domain walls.
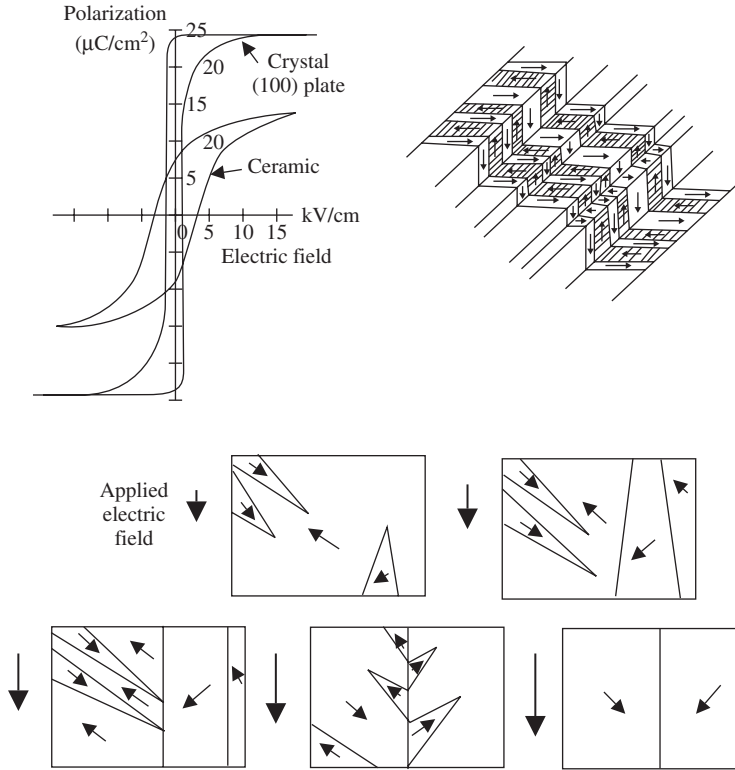
Fig. 16.14 Hysteresis loops for ferroelectric BaTiO$_3$ single crystals and ceramics. Near room temperature, the spontaneous polarization is 0.26 C/m^2. Typical domain structure and field-induced domain wall movements are shown below.

however, that involves the spontaneous polarization. As shown in Fig. 16.12 there is a substantial change in $P_{(s)}$ across 180° walls. Therefore the wall will be charged unless it is parallel to $P_{(s)}$ and to $-P_{(s)}$. For domains polarized along $\pm Z_3$, $(h\,k\,0)$ planes satisfy this criterion. Similar rules apply for 180° domain walls separating domains polarized along $\pm Z_1$ or $\pm Z_2$.

$$x_{(s)}^{I} = \begin{pmatrix} -x_s/2 \\ -x_s/2 \\ +x_s \\ 0 \\ 0 \\ 0 \end{pmatrix}, \quad x_{(s)}^{II} = \begin{pmatrix} -x_s/2 \\ -x_s/2 \\ +x_s \\ 0 \\ 0 \\ 0 \end{pmatrix}, \quad \Delta x_{(s)} = \begin{pmatrix} 0 \\ 0 \\ 0 \\ 0 \\ 0 \\ 0 \end{pmatrix},$$

$$P_{(s)}^{I} = \begin{pmatrix} 0 \\ 0 \\ P_s \end{pmatrix}, \quad P_{(s)}^{II} = \begin{pmatrix} 0 \\ 0 \\ -P_s \end{pmatrix}, \quad \Delta P_{(s)} = \begin{pmatrix} 0 \\ 0 \\ 2P_s \end{pmatrix},$$

$$\Delta G = -2P_{(s)3}E_3 \Rightarrow \text{Driving force.}$$

The 90° domains in BaTiO$_3$ (Fig. 16.13) show both ferroelectric and ferroelastic behavior. Differences in spontaneous polarization and spontaneous strain for neighboring domains are both substantial. The spontaneous polarization is measured from hysteresis loops (Fig. 16.14) while the spontaneous strain can be estimated from lattice parameters. For a tetragonal crystal, $\Delta x_{(s)} = (c - a)/\sqrt[3]{a^2c}$.

$$x^{\mathrm{I}}_{(s)} = \begin{pmatrix} -x_s/2 \\ -x_s/2 \\ +x_s \\ 0 \\ 0 \\ 0 \end{pmatrix}, \quad x^{\mathrm{III}}_{(s)} = \begin{pmatrix} -x_s/2 \\ +x_s \\ -x_s/2 \\ 0 \\ 0 \\ 0 \end{pmatrix}, \quad \Delta x_{(s)} = \begin{pmatrix} 0 \\ -3x_{(s)}/2 \\ +3x_{(s)}/2 \\ 0 \\ 0 \\ 0 \end{pmatrix},$$

$$P^{\mathrm{I}}_{(s)} = \begin{pmatrix} 0 \\ 0 \\ P_s \end{pmatrix}, \quad P^{\mathrm{III}}_{(s)} = \begin{pmatrix} 0 \\ P_s \\ 0 \end{pmatrix}, \quad \Delta P_{(s)} = \begin{pmatrix} 0 \\ -P_s \\ +P_s \end{pmatrix}$$

$$\Delta G = -P_s(E_3 - E_2) - \frac{3x_s}{2}(X_3 - X_2).$$

The 90° walls are parallel to {110} planes to minimize strain mismatch. Because of the c/a strain ratio, 90° domains are actually 90° 36′ apart resulting in slightly tapered domain wall configurations, and are optically distinguishable in a polarizing microscope.

There are many other ferroelectric oxides with the perovskite, tungsten bronze, pyrochlore, and bismuth titanate layer structure (Table 16.5). Compared with other oxides, all have high dielectric constants, high refractive indices, and large electromechanical coupling coefficients, and all contain corner-linked octahedral networks of Ti^{4+}, Nb^{5+}, or other d° ions. These transition-metal elements are the highly polarizable "active" ions promoting ferroelectricity, and the high permittivities and piezoelectric constants required for transducers and capacitors. With reference to the periodic system, there are two major groups of active ions, and both are near electronic "crossover" points where different types of atomic orbitals are comparable in energy and where hybrid bond formation is prevalent. The first group typified by Ti^{4+}, Nb^{5+}, Ta^{5+}, and W^{6+}, consists of d° ions octahedrally coordinated to oxygen. For Ti^{4+} the electronic crossover involves the 3d, 4s, and 4p orbitals, which combine

Table 16.5 Ferroelectric crystals, Curie temperatures (T_c), additional phase transitions (T_t), spontaneous polarization, and symmetry groups

Compound	Symmetry	T_c (K)	T_t (K)	$P_{(s)}$ (C/m²)
$Ba_2NaNb_5O_{15}$	4/*mmm* F 4*mm* F *mm*2	858	573	
$BaTiO_3$	*m3m* F 4*mm* F *mm*2 F 3*m*	408	278,183	0.26
$Bi_4Ti_3O_{12}$	4/*mmm* F *m*	949		
$(CH_2NHCOOH)_3H_2SO_4$	2/*m* F 2	322		0.031
$Gd_2(MoO_4)_3$	$\bar{4}$2*m* F *mm*2	432		0.0017
KH_2PO_4	$\bar{4}$2*m* F *mm*2	122		0.048
$KNa(C_4H_4O_6) \cdot 4H_2O$	222 F 2 F 222	297	255	0.025
$KNbO_3$	*m3m* F 4*mm* F *mm*2 F 3*m*	708	498,263	0.30
$LiNbO_3$	$\bar{3}$*m* F 3*m*	1473		0.71
$LiTaO_3$	$\bar{3}$*m* F 3*m*	938		0.50
$NaNO_2$	*mmm* F *mm*2	437		0.085
$Pb_5Ge_3O_{11}$	$\bar{6}$ F 3	450		
$Pb_3MgNb_2O_9$	*m3m* F 3*m*	263		
$PbNb_2O_6$	4/*mmm* F *mm*2	843		
$PbTiO_3$	*m3m* F 4*mm*	763		0.57
SbSI	*mmm* F *mm*2	295		0.25
$Sr_2Nb_2O_7$	*mmm* F *mm*2	1623		

with the σ and π orbitals of its six O^{2-} neighbors to form a number of molec-ular orbitals for the $(TiO_6)^{8-}$ complex. The bond energy of the complex can be lowered by distorting the octahedron to a lower symmetry. This leads to molecular dipole moments and ferroelectric and ferroelastic hysteresis as the dipoles reorient under electric fields or mechanical stress. A second group of active elements contributing to polar distortions in oxide dielectrics are the lone-pair ions having two electrons outside a closed shell in an asymmetric hybrid orbital. Among oxides, the most important of these lone-pair ions are Pb^{2+} and Bi^{3+} that are found in a number of ferroelectrics ($PbTiO_3$, $PbNb_2O_6$, $Bi_4Ti_3O_{12}$) with high Curie temperatures. In many of these compounds, Pb^{2+} and Bi^{3+} are in pyramidal coordination with oxygen and therefore contribute to the spontaneous polarization.

Among the other ferroelectric compounds listed in Table 16.5, there are other molecular mechanisms for ferroelectricity. Hydrogen bonding plays a key role in Rochelle Salt, triglycine sulfate, and potassium dihydrogen phosphate. In many water-soluble ferroelectric crystals such as these, the transition from the paroelectric state above T_c to the low-temperature ferroelectric state is essentially an order—disorder phenomenon. Above the transition, protons are statistically distributed in double potential wells. Below T_c they freeze into ordered positions, lowering the symmetry and creating ferroelectric domains.

Problem 16.4
Bismuth titanate, $Bi_4Ti_3O_{12}$, is ferroelectric below the Curie temperature of 949 K where it changes from tetragonal ($4/mmm$) to monoclinic (m). At room temperature, the components of spontaneous polarization are $P_{(s)1} = 0.50$, $P_{(s)2} = 0$, and $P_{(s)3} = 0.05$ C/m^2 along the principal axes. Make plots of the spontaneous polarization as a function of direction for the eight domain states, remembering that Z_1 and Z_2 are equivalent to one another in the high temperature structure.

The spontaneous strains are $x_{(s)11} = -x_{(s)22} = 0.0068$. All other components are zero or near zero. Write out the equation for the difference in free energy between two domain states (ΔG) and determine the components of electric field and mechanical stress that will move the domain wall between them.

16.6   Secondary ferroics: Ferrobielectricity and ferrobimagnetism

Examples of the six types of secondary ferroic phenomena are listed in Table 16.1. Ferrobielectricity is a secondary ferroic effect arising from field-induced electric polarization, rather than spontaneous polarization as in a ferroelectric. Switching between orientation states occurs because of differ-ences in the dielectric permittivity tensor. Permittivity is a secondary tensor like strain and magnetic susceptibility. Any orientation states differing in spon-taneous strain will also differ in both electric and magnetic susceptibility. Therefore all ferroelastics are potentially ferrobielectric and ferrobimagnetic.

Ferrobielectricity can be expected in nonpolar crystals with mimetic twin-ning and substantial dielectric anisotropy. Antiferroelectric materials such as $NaNbO_3$ and $SrTiO_3$ are promising candidates because the dielectric